Check for updates

Enhanced production of optical (S)-acetoin by a recombinant *Escherichia coli* whole-cell biocatalyst with NADH regeneration†

Jian-Xiu Li, [ID] [ab] Yan-Yan Huang, [b] Xian-Rui Chen, [b] Qi-Shi Du, [ID] [b] Jian-Zong Meng, [a] Neng-Zhong Xie [ID] *[b] and Ri-Bo Huang*[ab]

Acetoin is an important platform chemical with a variety of applications in foods, cosmetics, chemical synthesis, and especially in the asymmetric synthesis of optically active pharmaceuticals. It is also a useful breath biomarker for early lung cancer diagnosis. In order to enhance production of optical (S)-acetoin and facilitate this building block for a series of chiral pharmaceuticals derivatives, we have developed a systematic approach using *in situ*-NADH regeneration systems and promising diacetyl reductase. Under optimal conditions, we have obtained 52.9 g L^{-1} of (S)-acetoin with an enantiomeric purity of 99.5% and a productivity of 6.2 g $(L\ h)^{-1}$. The results reported in this study demonstrated that the production of (S)-acetoin could be effectively improved through the engineering of cofactor regeneration with promising diacetyl reductase. The systematic approach developed in this study could also be applied to synthesize other optically active α-hydroxy ketones, which may provide valuable benefits for the study of drug development.

1. Introduction

Enantiomeric α-hydroxy ketones are important pharmaceutical intermediates, widely applied in antifungal agents, antitumor antibiotics, antidepressants, farnesyl transferase inhibitors and selective inhibitors of amyloid-β protein production.[1–3] Acetoin (3-hydroxy-2-butanone), the smallest natural chiral α-hydroxy ketone, is a popular flavor additive, preservative, plant growth promoter and breath biomarker of early lung cancer, and is identified as one of the top 30 potential building blocks.[4–7] This four-carbon compound has one chiral center in the molecule and therefore exists as two stereoisomers, (R)-acetoin and (S)-acetoin.[8,9] With FEMA no. 2008, acetoin is a substance generally recognized as safe (visit https://ntp.niehs.nih.gov/ for toxicity and related information). Acetoin and its isomers are widely applied in foods, cosmetics, chemical synthesis, especially in asymmetric synthesis of optically active pharmaceuticals and liquid crystals.[10,11] Its derivate, 4-chloro-4,5-dimethyl-1,3-dioxolan-2-one, has been extensively utilized in modifying

antibiotics to synthesize optically active drugs, which could enhance drug targeting properties and reduce side effects.[12,13]

Native microorganisms generally produce acetoin as a mixture of two stereoisomers, in which (R)-acetoin is predominant and (S)-acetoin exists as a minor by-product, leading to very low yield of (S)-acetoin and high cost of chiral separation.[14–16] Liu *et al.* developed an engineered *Lactococcus lactis* to produce (S)-acetoin from glucose.[17] However, the nonenzymatic oxidative decarboxylation of α-acetolactate to diacetyl occurred spontaneously and inefficiently, the engineered strain could only produce 5.8 g L^{-1} of (S)-acetoin with a productivity of 0.19 g $(L\ h)^{-1}$. Several attempts to produce (S)-acetoin by using purified enzymes have been reported previously. According to Loschonsky *et al.*, cyclohexane-1,2-dione hydrolase formed (S)-acetoin with a 95% enantiomeric excess from 23 mM substrate by homocoupling of acetaldehyde.[18] In 2013, Gao *et al.* developed a two-enzymes coupling system, in which NADPH-dependent carbonyl reductase reduced diacetyl to produce (S)-acetoin, and glucose dehydrogenase was used to regenerate NADPH. Under optimal conditions, 12.2 g L^{-1} of (S)-acetoin (enantiomeric purity: 96.9%) with a productivity of 9.8 g $(L\ h)^{-1}$ was produced.[19]

Recently, recombinant whole-cells have emerged as biocatalysts for (S)-acetoin production. He *et al.*[20] described a whole-cell biocatalytic process with a high yield by recombinant *E. coli* cells co-expressing (2R,3R)-2,3-butanediol dehydrogenase (R,R-BDH), NADH oxidase and hemoglobin. The recombinant strain produced 72.4 g L^{-1} (S)-acetoin from a mixtures of 2,3-butanediol isomers. However, the enantiomeric purity of the product was

[a] State Key Laboratory for Conservation and Utilization of Subtropical Agro-Bioresources, Life Science and Biotechnology College, Guangxi University, 100 Daxue Road, Nanning, 530004, China. E-mail: xienengzhong@gxas.cn; guruace@ 163.com

[b] State Key Laboratory of No-Food Biomass and Enzyme Technology, National Engineering Research Center for No-Food Biorefinery, Guangxi Key Laboratory of Biorefinery, Guangxi Academy of Sciences, 98 Daling Road, Nanning, 530007, China

only 94.7% for the generation of (*R*)-acetoin. Since (*S*)-acetoin can be used to provide chiral groups in high-value pharmaceuticals or for liquid crystals, high optical purity (*i.e.*, over 98.0%) is particularly required. Gao *et al.* developed a whole-cell biocatalytic process for (*S*)-acetoin production by over-expressing diacetyl reductase (DAR) in *E. coli*.[12] When diacetyl and glucose were used as substrate and co-substrate respectively, the recombinant whole-cells could produce 39.4 g L^{-1} of (*S*)-acetoin in 20 h. Since diacetyl is a prochiral compound that can be produced by chemical synthesis or microbial fermentation, it is a preferred substrate for optical (*S*)-acetoin.[12,19,21,22] However, two problems still need to be solved. First, due to the high concentration of intracellular DAR, the endogenous cofactor regeneration system of *E. coli* is typically not sufficiently efficient,[23,24] limiting the titer and productivity of (*S*)-acetoin; second, organic acids (*e.g.* acetic acid and lactic acid) produced during glucose metabolism make product recovery difficult and increase glucose consumption.[25]

In this study, an efficient and economical process was developed for optical (*S*)-acetoin production from diacetyl. As shown in Fig. 1, two *in situ*-NADH regeneration systems were introduced into *E. coli* and determined their effectiveness in (*S*)-acetoin production. DAR genes from several species were codon-optimized and over-expressed to screen for a promising DAR with high stereoselectivity, specific activity and stability. Finally, a series of whole-cell biocatalytic reactions were performed to achieve high (*S*)-acetoin production.

2. Materials and methods

2.1 Chemicals

(2*S*,3*S*)-2,3-Butanediol (99.0%) and *meso*-2,3-butanediol (98.0%) were obtained from ACROS (Geel, Belgium). (2*R*,3*R*)-2,3-Butanediol (97.0%), acetoin (99.0%), NADH, and NAD$^+$ were obtained from Sigma (St Louis, USA). Diacetyl (99.0%) was obtained from Aladdin (Shanghai, China). PCR primers were synthesized by Sangon (Shanghai, China) and DNA sequencing was performed by Genscript (Nanjing, China). Yeast extract and peptone were obtained from Oxoid (Hampshire, UK).

2.2 Bacterial strains and vectors

The strains and vectors used in the present study are listed in Table 1. *E. coli* DH5α and *E. coli* BL21(DE3) were used for gene cloning and protein expressing, respectively. The pET-28a(+) and pETDuet-1 were used for gene expression. Luria–Bertani medium (10 g L^{-1} peptone, 5 g L^{-1} yeast extract, and 10 g L^{-1} NaCl at pH 7.0) was used for *E. coli* cultivation and solidified with 1.5% agar, if necessary. Kanamycin and ampicillin were used at concentrations of 30 μg mL^{-1} and 100 μg mL^{-1}, respectively.

2.3 Synthesis of DAR genes and construction of co-expression systems

DNA manipulations were carried out using standard protocols.[26] The codons for the DAR genes, Kp*dar* from *K. pneumoniae*
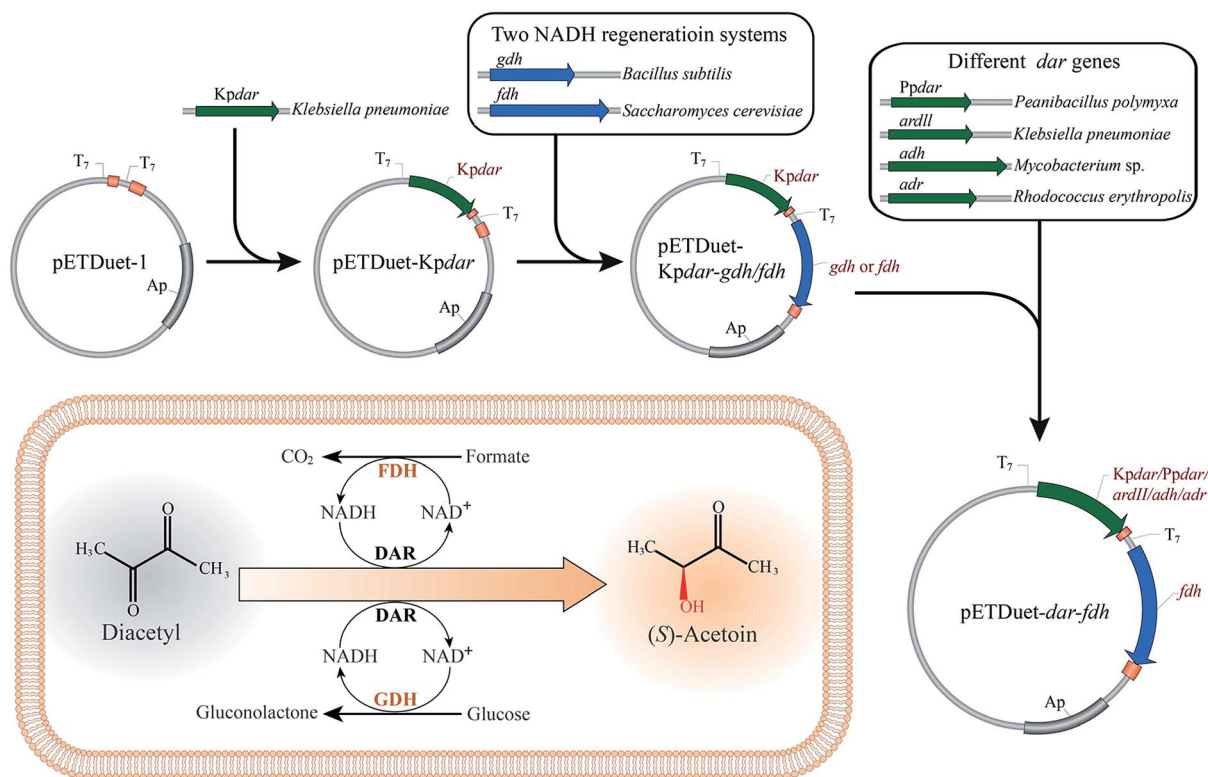

Fig. 1 Scheme for (*S*)-acetoin production from diacetyl using recombinant whole-cell biocatalysts with NADH regeneration systems. *dar*, the gene encoding diacetyl reductase (DAR); *gdh*, the gene encoding glucose dehydrogenase (GDH); *fdh*, the gene encoding formate dehydrogenase (FDH); Ap: the gene encoding ampicillin resistance.

Table 1 Strains and plasmids used in this study

Strain and plasmid	Genotype and properties	Source or reference
Strain		
E.coli DH5α	*supE44* △ *lacU169* (*φ80 lacZ* △ *M15*) *hsdR17 recA1 endA1 gyrA96 thi-1 relA1*	Novagen
E.coli BL21(DE3)	F^- *ompT hsdSB* (rB^-mB^-) *gal* (λ *c I 857 ind1 Sam7 nin5 lacUV5 T7gene1*) *dcm* (DE3)	Novagen
Plasmid		
pET-28a(+)	Overexpression vector; Kan^r	Novagen
pETDuet-1	Overexpression vector; Amp^r	Novagen
pET-28a(+)-Kp*dar*	Kp*dar* in pET-28a(+)	This work
pETDuet-*fdh*	*fdh* in pETDuet-1	This work
pETDuet-Kp*dar*	Kp*dar* in pETDuet-1	This work
pETDuet-Kp*dar-gdh*	Kp*dar* and *gdh* in pETDuet-1	This work
pETDuet-Kp*dar-fdh*	Kp*dar* and *fdh* in pETDuet-1	This work
pETDuet-Pp*dar-fdh*	Pp*dar* and *fdh* in pETDuet-1	This work
pETDuet-*ard* II-*fdh*	*ard* II and *fdh* in pETDuet-1	This work
pETDuet-*adh-fdh*	*adh* and *fdh* in pETDuet-1	This work
pETDuet-*adr-fdh*	*adr* and *fdh* in pETDuet-1	This work

CICC 10011 (GenBank accession no. HM113375.1), Pp*dar* from *P. polymyxa* DSM 365 (GenBank accession no. KT717931), *ard* II from *K. pneumoniae* 342 (GenBank accession no. CP000964.1), *adh* from *Mycobacterium* sp. B-009 (GenBank accession no. AB905197.1), and *adr* from *R. erythropolis* WZ010 (GenBank accession no. KC508606.1), were optimized and synthesized by Genscript (Nanjing, China), and then inserted into pETDuet-1 between the *Nco* I and *Sac* I sites to yield expression vectors. The formate dehydrogenase (FDH) gene *fdh* from *S. cerevisiae* (NCBI reference sequence NM_001183808.1), and Glucose dehydrogenase (GDH) gene *gdh* from *B. subtilis* (GenBank accession no. CP019663.1), were also synthesized with codon optimization. The *fdh* and *gdh* fragments were digested with *Nde* I and *Kpn* I, respectively. Then the fragments were ligated into the expression vectors that had been digested with the same restriction endonucleases. The co-expression plasmids were designated pETDuet-Kp*dar-gdh*, pETDuet-Kp*dar-fdh*, pET-Duet-Pp*dar-fdh*, pETDuet-*ard* II-*fdh*, pETDuet-*adh-fdh*, and pETDuet-*adr-fdh*, respectively.

2.4 Biocatalyst preparation and bioconversion conditions

The recombinant *E. coli* strains were cultivated at 37 °C and 180 rpm to OD_{600} of 0.6. According to preliminary experiments, recombinant genes expression was induced with 0.2 mM IPTG at 25 °C for 12 h. The cells were harvested by centrifugation at 6000 rpm and then washed twice with 0.85% NaCl. The cell pellet was resuspended in 100 mM phosphate buffer (pH 7.5) at a concentration of 20 $g_{(DCW)}$ L^{-1} and maintained at 4 °C. The dry cell weight (DCW) of *E. coli* was determined by converting the OD_{600} value with a coefficient of 0.275 $g_{(DCW)}$ per (LOD_{600}).[27]

A typical bioconversion reaction was carried out with 5.5 $g_{(DCW)}$ L^{-1} whole-cell biocatalyst in 50 mL flasks. A total of 10 mL

of the mixture was reacted in 100 mM phosphate buffer (pH 7.5) at 32 °C and 200 rpm for 2 h. (*S*)-Acetoin production by whole-cells co-expressing *fdh* with DAR genes was carried out using 15.0 g L^{-1} of diacetyl and 12.0 g L^{-1} of formate (only account molecular mass of formate ion). For (*S*)-acetoin production by whole-cells co-expressing Kp*dar* with *gdh*, 15.0 g L^{-1} of diacetyl and 30.0 g L^{-1} of glucose were required.

2.5 Optimization of the reaction conditions

To achieve a high conversion efficiency, the pH (5.5, 6.0, 6.5, 7.0, 7.5, or 8.0), temperature (28 °C, 32 °C, 36 °C, 40 °C, or 45 °C), molar ratio of formate to diacetyl (0.6, 0.8, 1.0, 1.2, 1.6, or 2.0), and shaking speed (75 rpm, 100 rpm, 125 rpm, 150 rpm, or 175 rpm) were investigated in turn. An initial bioconversion was reacted in 100 mM phosphate buffer at 32 °C and 200 rpm for 2 h. The concentrations of cell, diacetyl and formate in the reaction was 5.5 $g_{(DCW)}$ L^{-1}, 15 g L^{-1} and 12 g L^{-1}, respectively.

2.6 Fed-batch biotransformation

Fed-batch biotransformation was carried out in a 10 mL mixture at 40 °C and 125 rpm. The initial concentrations of diacetyl and whole-cell biocatalyst were 15.0 g L^{-1} and 5.5 $g_{(DCW)}$ L^{-1}, respectively. The ratio of formate to diacetyl was 1.2, and the pH was 6.5. During bioconversion, diacetyl was fed at intervals to maintain its concentration at 5.0–15.0 g L^{-1}, and pH was adjusted to 6.5 by formic acid. At the same time, small amounts of whole cell biocatalyst were added at the interval time, until the whole cell concentration reached to 11.0 $g_{(DCW)}$ L^{-1}.

2.7 Purification of KpDAR

E. coli BL21(DE3) carrying plasmid pET-28a (+)-Kp*dar* was cultivated at 37 °C and 200 rpm to OD_{600} of 0.6, and then 0.4 mM IPTG was added to the culture at 20 °C for 12 h. The culture was centrifuged at 6000 rpm, and the cell pellet was resuspended in buffer (pH 7.4; 20 mM potassium phosphate, 500 mM sodium chloride, 20 mM imidazole, 1 mM DTT, 0.1 mM PMSF, and 10% glycerol). Cells were disrupted by sonication in an ice bath and centrifuged at 12 000 rpm for 30 min at 4 °C. The Kp*dar* was purified by HisTrap HP column (GE Healthcare) and detected by SDS-PAGE.

2.8 Assays for DARs, GDH and FDH activities

Crude proteins were extracted from recombinant *E. coli* using BugBuster Master Mix reagent (Novagen). Enzyme activities were determined by monitoring the change in optical density at 340 nm corresponding to the reduction of NAD^+ or oxidation of NADH ($\varepsilon_{340} = 6.22$/mM cm) using a UV/visible spectrophotometer (DU800, Beckman). One unit of DAR activity was defined as the amount of enzyme that consumed 1 μmol of NADH per min. The reaction mixture contained 5 mM diacetyl and 0.2 mM NADH in 100 mM phosphate buffer (pH 6.5). One unit of GDH or FDH activity was defined as the amount of enzyme that produced 1 μmol of NADH per min. The reaction mixture contained 5 mM substrate (glucose or formate) and 0.2 mM NAD^+ in 100 mM phosphate buffer (pH 6.5). The reaction solution for the

KpDAR reduction assay contained 5 mM of ketone substrate and 0.2 mM of NADH in 100 mM phosphate buffer and for KpDAR oxidation contained 5 mM of alcohol substrate and 0.2 mM of NAD$^+$ in 100 mM phosphate buffer. Protein concentrations were determined *via* the Bradford method using bovine serum albumin as a standard.

2.9 Analytical methods

The concentrations of diacetyl, acetoin, and 2,3-butanediol in the supernatant were determined using a gas chromatography (GC) system (Agilent 7890A) equipped with a polar column (Phenomenex ZB-WAX plus, 0.32 mm × 0.25 μm × 30 m). The injector and detector temperatures were both 250 °C. The column oven temperature was maintained at 100 °C for 1 min, then increased to 180 °C at a rate of 20 °C min^{-1}, finally maintained at 180 °C for 3 min. (*R*)-Acetoin and (*S*)-acetoin in the supernatant were extracted using ethyl acetate and then measured by the GC system (Agilent 7890A) equipped with a chiral column (Agilent Cyclosil-B, 0.32 mm × 0.25 μm × 30 m). The temperatures of injector and detector were both 240 °C. The column oven temperature was maintained at 100 °C for 1 min and increased to 120 °C at a rate of 10 °C min^{-1}. Then, it was increased to 130 °C at a rate of 6 °C min^{-1} and finally to 230 °C at a rate of 20 °C min^{-1}. The enantiomeric purity of (*S*)-acetoin was defined as [S]/([S] + [R]) × 100%, where [R] and [S] represented the concentrations of (*R*)-acetoin and (*S*)-acetoin, respectively. Formate and other organic acids concentration were analyzed using high-performance liquid chromatography (HPLC) system (Dionex UltiMate 3000) equipped with a Carbomix H-NP column (Sepax, 7.8 × 300 mm). The analysis was conducted at 55 °C with a mobile phase of 2.5 mM H_2SO_4 at a flow rate of 0.6 mL min^{-1}.

3. Results and discussion

3.1 Construction of different whole-cell biocatalysts by cofactor engineering

Redox balance plays an important role for cell growth and cellular metabolism.[28] When heterogeneous oxidoreductases are overexpressed, the endogenous cofactor regeneration system is typically not sufficiently efficient.[23] GDH and FDH are widely used for *in situ*-cofactor regeneration.[25,29–31] To investigate their effect on (*S*)-acetoin production, *gdh* gene from *Bacillus subtilis*[32] and *fdh* gene from *Saccharomyces cerevisiae*[33] were synthesized after codon optimization (see ESI Table S1†) by GenScript (Nanjing, China) and co-expressed with DAR gene in *E. coli* BL21(DE3). To obtain a promising DAR, five DAR genes from several species were codon-optimized (see ESI Table S1†) and co-expressed with *fdh* or *gdh* to compare for (*S*)-acetoin synthesis. Recombinant DARs were detected by SDS-PAGE (see ESI Fig. S1†).

Batch biotransformation was conducted to evaluate the performance of two NADH regeneration systems with formate or glucose as co-substrate. As shown in Table 2, the conversion rate was low, obtained by *E. coli* BL21/pETDuet-Kp*dar* with single expression of KpDAR, and the final titer of (*S*)-acetoin was only 0.8 g L^{-1} with an enantiomeric purity of 89.3% and productivity of 0.4 g (L h)$^{-1}$. The crude extract enzyme of *E. coli* BL21/pET-Duet-Kp*dar-gdh* showed a KpDAR activity of 33.4 U mg^{-1} and a GDH activity of 16.3 U mg^{-1}. When introducing the GDH/glucose system, the titer of (*S*)-acetoin increased to 4.3 g L^{-1} with an enantiomeric purity of 94.4% and productivity of 2.2 g (L h)$^{-1}$ by *E. coli* BL21/pETDuet-Kp*dar-gdh*. Introduction of the FDH/formate system resulted in a higher (*S*)-acetoin titer, productivity and enantiomeric purity. 6.7 g L^{-1} of (*S*)-acetoin was obtained with an enantiomeric purity of 99.6% and productivity of 3.4 g (L h)$^{-1}$ by *E. coli* BL21/pETDuet-Kp*dar-fdh*. Crude extract of this recombinant strain showed a KpDAR activity of 34.9 U mg^{-1} and a FDH activity of 0.45 U mg^{-1}, while *E. coli* BL21/pETDuet-Kp*dar* showed a KpDAR activity of 79.0 U mg^{-1}.

Acetoin biosynthesis initiates with the condensation of two pyruvate molecules to yield one α-acetolactate, then yield (*R*)-acetoin by decarboxylases or diacetyl upon spontaneous decarboxylation.[24,34,35] Diacetyl can be further converted into (*R*)-acetoin or (*S*)-acetoin by DAR or BDH. Liang *et al.* reported that *E. coli* has an endogenous acetoin/2,3-butanediol pathway and glucose can be metabolized to acetoin by diacetyl-dependent endogenous system.[24] In our study, the enantiomeric purity of (*S*)-acetoin produced by *E. coli* BL21/pETDuet-Kp*dar-gdh* with glucose as co-substrate was low (94.4%), indicating that (*R*)-acetoin was produced by the intrinstic acetoin/2,3-butanediol pathway of *E. coli.* While in FDH/formate system, only a trace amount of (*R*)-acetoin was detected for the absence of glucose, and the enantiomeric purity of (*S*)-acetoin can reach to 99.6% by *E. coli* BL21/pETDuet-Kp*dar-fdh*.

Low-molecular-weight formate has similar price with glucose. Regeneration of 1 mol of NADH requires only 45 g of formate comparing 172 g of glucose, indicating that the reducing equivalent capacity of formate is approximately four-fold higher than that of glucose.[30] In addition, glucose can be metabolized to acetic acid, lactic acid by *E. coli*, further

Table 2 The products of batch bioconversion with different DARs and cofactor regeneration systems

Strain	(*S*)-Acetoin (g L^{-1})	Productivity (g (L h)$^{-1}$)	Enantiomeric purity (%)
E. coli BL21/pETDuet-Kp*dar*	0.8 ± 0.01	0.4	89.3 ± 0.97
E. coli BL21/pETDuet-Kp*dar-gdh*	4.3 ± 0.12	2.2	94.4 ± 0.79
E. coli BL21/pETDuet-Kp*dar-fdh*	6.7 ± 0.08	3.4	99.6 ± 0.08
E. coli BL21/pETDuet-Pp*dar-fdh*	3.2 ± 0.04	1.6	95.9 ± 0.77
E. coli BL21/pETDuet-*ard* II-*fdh*	1.2 ± 0.02	0.6	54.5 ± 0.07
E. coli BL21/pETDuet-*adh-fdh*	1.8 ± 0.03	0.4	90.2 ± 0.09
E. coli BL21/pETDuet-*adr-fdh*	5.5 ± 0.15	2.8	98.5 ± 0.19

increasing glucose consumption.[25] FDH catalyses the conversion of formate to CO_2 with no organic acid products, reducing the cost associated with the co-substrate and downstream processing.[30,31,36] Considering the higher enantiomeric purity and titter, lower cost of the co-substrate, and easier purification, the FDH/formate system would significantly reduce total cost of (S)-acetoin production.

When co-expressing *fdh* with other DAR genes including Pp*dar*, *ard* II, *adr*, or *adh*, all resulting biocatalysts produced (S)-acetoin, but the titer and enantiomeric purity of (S)-acetoin varied widely (Table 2). Because *E. coli* BL21/pETDuet-Kp*dar-fdh* showed the best performance in terms of both titer and enantiomeric purity among all recombinant strains, this strain together with KpDAR was used for subsequent analysis.

3.2 Purification and characterization of KpDAR

KpDAR was purified by Ni-affinity chromatography and confirmed by SDS-PAGE. The purified KpDAR showed single bands about 28 kDa on the SDS-PAGE (see ESI Fig. S2†). Oxidation and reduction reactions were conducted to investigate the substrate specificities of KpDAR (see ESI Table S2†). KpDAR had clear activities towards diacetyl, (R)/(S)-acetoin and *meso*-2,3-butanediol with NADH/NAD$^+$ as the cofactor. Diacetyl was the best substrate in the ketone reduction reactions. The

specific activity of purified KpDAR towards diacetyl was up to 2887.6 U mg^{-1}. *meso*-2,3-Butanediol was the best substrate in the alcohol oxidation reactions, while very low activity was observed with (R)/(S)-acetoin, (2S,3S)-2,3-butanediol and (2R,3R)-2,3-butanediol.

3.3 Optimization of the reaction conditions

The reaction conditions for (S)-acetoin production were optimized to increase the efficiency of the whole-cell biocatalysis. Because reaction pH and temperature are two important parameters that strongly influence enzyme activities and cellular maintenance, the effects of pH and temperature on whole-cell biocatalysis were first investigated. As shown in Fig. 2a, the titer (9.19 g L^{-1}) and yield (59.9%) of (S)-acetoin was high at pH 6.5. Under more acidic or alkaline conditions, the yield of the transformation decreased. As shown in Fig. 2b, the optimal temperature was found at 40 °C, and the yield of (S)-acetoin increased to 67.8%.

The substrate specificities of KpDAR indicated that KpDAR not only showed a high catalytic efficiency toward diacetyl, but also exhibited acetoin reductase activity (see ESI Table S2 and Fig. S3†). Both reductions of diacetyl and (S)-acetoin are accomplished with stoichiometric amounts of NADH consumption. Through manipulating the level of NADH/NAD$^+$,
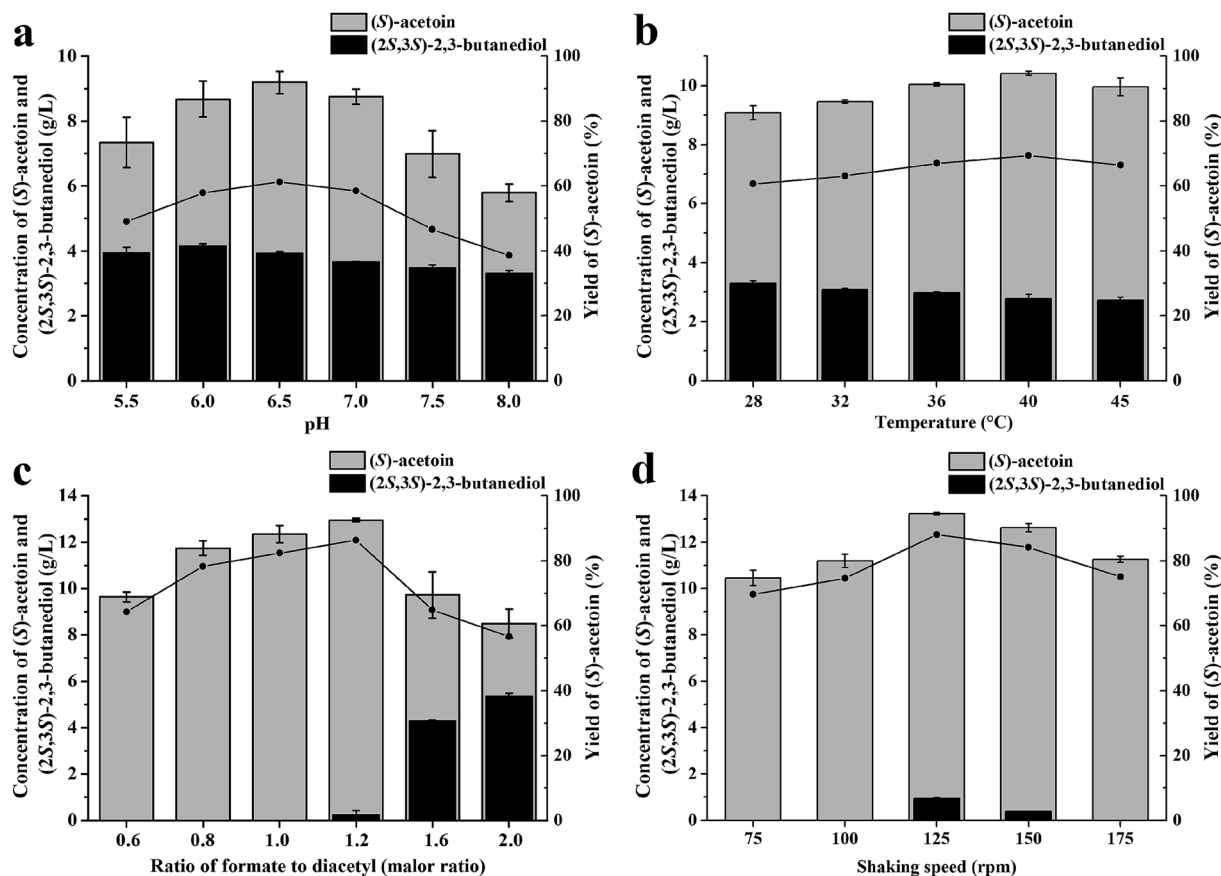

Fig. 2 Optimization of biocatalysis conditions. (a) pH; (b) temperature; (c) ratio of formate to diacetyl; (d) shaking speed. (●) Yield of (S)-acetoin. Error bars indicate standard deviations (n = 3).
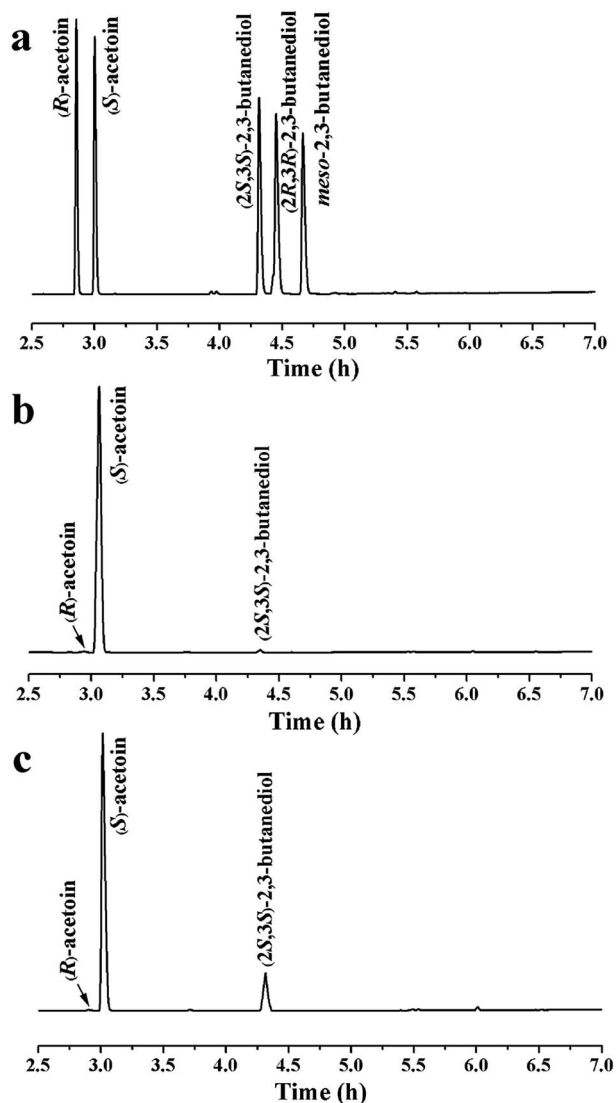
Fig. 3 Chiral-column GC analyses of products produced by whole-cell of *E. coli* BL21/pETDuet-Kp*dar-fdh*. (a) Standard samples of pure stereoisomers; (b) sample from batch bioconversion by *E. coli* BL21/pETDuet-Kp*dar-fdh*; (c) sample from fed-batch bioconversion by *E. coli* BL21/pETDuet-Kp*dar-fdh*. Samples were extracted using ethyl acetate and isoamyl alcohol was used as the internal standard.

production of (*S*)-acetoin can be improved.[25] Thus, to enhance (*S*)-acetoin production, the concentration of formate should be optimized. As shown in Fig. 2c, when the molar ratio of formate to diacetyl was low, increasing the concentration of formate effectively increased the efficiency of (*S*)-acetoin production. When the molar ratio was 1.2, (*S*)-acetoin production reached its maximum level (12.96 g L^{-1}) with a yield of 84.4%. Further increasing formate concentration to provide more NADH resulted in accumulation of (2*S*,3*S*)-2,3-butanediol, thus decreased the final yield of (*S*)-acetoin.

Oxygen supply can significantly affect the ratio of NADH/NAD$^+$. Different oxygen supplies were investigated by varying the shaking speeds, and the optimal shaking speed was 125 rpm, as shown in Fig. 2d. Under optimal conditions, 13.2 g

L^{-1} of (*S*)-acetoin was accumulated from 15.0 g L^{-1} of diacetyl with a productivity of 6.6 g (L h)$^{-1}$ (Fig. 2d). The yield of (*S*)-acetoin was 86.0% and the enantiomeric purity was 99.6% (Fig. 3a and b).

3.4 Fed-batch biotransformation

Diacetyl is toxic to recombinant *E. coli*,[12,32] and therefore fed-batch processes should be performed to avoid substrate inhibition and achieve high product concentration.[37] In this study, fed-batch biotransformation was conducted with an initial diacetyl concentration of 15.0 g L^{-1}, while feeding small amounts of diacetyl and formate (ratio of formate to diacetyl approximately 1.2) at 1 h intervals. After 8.5 h of reaction, 52.9 g L^{-1} of (*S*)-acetoin was accumulated from 81.4 g L^{-1} of diacetyl with an enantiomeric purity of 99.5% (Fig. 3a and c) and productivity of 6.2 g (L h)$^{-1}$ (Fig. 4). The titer and productivity were new records on high optical (*S*)-acetoin (enantiomeric purity ≥ 98.0%) production to our knowledge. In addition, 15.6 g L^{-1} of (2*S*,3*S*)-2,3-butanediol was obtained (Fig. 4). It should be pointed out that this optical active compound is also a building block in the chiral synthesis,[20] and could be separated from (*S*)-acetoin by distillation for their different boiling points. No *meso*-2,3-butanediol, (2*R*,3*R*)-2,3-butanediol or organic acids were detected.

According to Liu *et al.*, (*S*)-acetoin was effectively produced by biocatalytic resolution of the mixture of *meso*-2,3-butanediol and (2*S*,3*S*)-2,3-butanediol by the resting cells of *B. subtilis* 168, in which *meso*-2,3-butanediol was converted to (*S*)-acetoin.[38] However, the enantiomeric purity of the product (*S*)-acetoin was low (96.2%) for the generation of (*R*)-acetoin, which may be due to the complex metabolic network of *B. subtilis*. Gao *et al.* reported that whole-cells of recombinant *E. coli* over-expressing DAR could be used to produced relatively high concentration of (*S*)-acetoin (39.4 g L^{-1}) from diacetyl.[12] However, the enantioselective reduction of one diacetyl molecule to form (*S*)-acetoin consumes one NADH/NADPH molecule as an electron
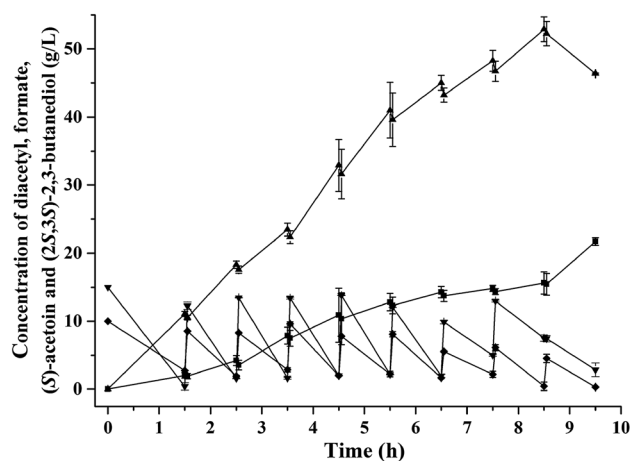

Fig. 4 Production of optical (*S*)-acetoin by *E. coli* BL21/pETDuet-Kp*dar-fdh* in fed-batch bioconversion. (▲) (*S*)-Acetoin, (■) (2*S*,3*S*)-2,3-butanediol, (▼) diacetyl, (◆) formate. Error bars indicate standard deviations (*n* = 3).

donor, while generating $NAD^+/NADP^+$.[19,39] Once the DAR level is no longer limiting, the NADH/NADPH levels become limiting. Thus, it is particularly important to construct an efficient cofactor regeneration system to further increase the productivity.

In the present study, DARs from several species were codon-optimized and compared for (S)-acetoin synthesis, and two typical *in situ*-cofactor regeneration systems were introduced into recombinant *E. coli*. In batch biotransformation, co-expressing KpDAR with FDH resulted in 8.4-fold increase in titer, with enantiomeric purity of 99.6%. Compared with the results achieved previously using glucose as a co-substrate,[12] co-expressing KpDAR with FDH improved the (S)-acetoin concentration from 39.4 g L^{-1} to 52.9 g L^{-1} and productivity from 2.0 g $(L\ h)^{-1}$ to 6.2 g $(L\ h)^{-1}$ in fed-batch biotransformation, indicating that the NADH level of *E. coli* was maintained appropriately by introduced FDH regeneration system. Thus, engineering of cofactor regeneration, together with a promising diacetyl reductase, can effectively improve the production of (S)-acetoin.

4. Conclusions

In this study, we developed an efficient and economical process for high-value chiral (S)-acetoin production from diacetyl. Two *in situ*-NADH regeneration systems were applied to improve the production of (S)-acetoin, and five DARs from several species were also compared for (S)-acetoin synthesis. Under the optimal conditions, 52.9 g L^{-1} of (S)-acetoin was produced with an enantiomeric purity of 99.5% and a productivity of 6.2 g $(L\ h)^{-1}$; the titer and productivity were new records on high optical (S)-acetoin (enantiomeric purity $\geq$ 98.0%) production to our knowledge. The systematic approach developed in this study could also be applied to synthesize other optically active α-hydroxy ketones.

Conflicts of interest

There are no conflicts to declare.

Acknowledgements

References

1 T. Tanaka, M. Kawase and S. Tani, *Bioorg. Med. Chem.*, 2004, **12**, 501–505.

2 O. B. Wallace, D. W. Smith, M. S. Deshpande, C. Polson and K. M. Felsenstein, *Bioorg. Med. Chem.*, 2003, **13**, 1203–1206.

3 Q. K. Fang, Z. X. Han, P. Grover, D. Kessler, C. H. Senanayake and S. A. Wald, *Tetrahedron: Asymmetry*, 2000, **11**, 3659–3663.

4 G. Song, T. Qin, H. Liu, G. B. Xu, Y. Y. Pan, F. X. Xiong, K. S. Gu, G. P. Sun and Z. D. Chen, *Lung Cancer*, 2010, **67**, 227–231.

5 X. A. Fu, M. X. Li, R. J. Knipp, M. H. Nantz and M. Bousamra, *Cancer Med.*, 2014, **3**, 174–181.

6 T. A. Werpy and G. Petersen, *Top value added chemicals from biomass: volume I - results of screening for potential candidates from sugars and synthesis gas*, US Department of Energy, 2004.

7 Z. J. Xiao and J. R. Lu, *Biotechnol. Adv.*, 2014, **32**, 492–503.

8 X. Ji, H. Huang and P. Ouyang, *Biotechnol. Adv.*, 2011, **29**, 351–364.

9 T. W. Yang, Z. M. Rao, X. Zhang, M. J. Xu, Z. H. Xu and S. T. Yang, *Crit. Rev. Biotechnol.*, 2017, **37**, 990–1005.

10 Q. Xu, L. Xie, Y. Li, H. Lin, S. Sun, X. Guan, K. Hu, Y. Shen and L. Zhang, *J. Chem. Technol. Biotechnol.*, 2015, **90**, 93–100.

11 S. Saito, H. Inoue and K. Ohno, EP0409234, EP Patent, 1991.

12 J. Gao, Y. Y. Xu, F. W. Li and G. Ding, *Lett. Appl. Microbiol.*, 2013, **57**, 274–281.

13 Y. Peng and S. Z. Chen, *Fine Chem. Intermed.*, 2002, **32**, 20–21.

14 S. Ui, M. Odagiri, A. Mimura, H. Kanai, T. Kobayashi and T. Kudo, *J. Ferment. Bioeng.*, 1996, **81**, 386–389.

15 Z. J. Xiao, P. H. Liu, J. Y. Qin and P. Xu, *Appl. Microbiol. Biotechnol.*, 2007, **74**, 61–68.

16 Z. Z. Cui, Y. F. Mao, Y. J. Zhao, C. Chen, Y. J. Tang, T. Chen, H. W. Ma and Z. W. Wang, *J. Chem. Technol. Biotechnol.*, 2018, DOI: 10.1002/jctb.5702.

17 J. Liu, C. Solem and P. R. Jensen, *Biotechnol. Bioeng.*, 2016, **113**, 2744–2748.

18 S. Loschonsky, S. Waltzer, B. Volker and P. M. Müller, *Chemcatchem*, 2014, **6**, 969–972.

19 C. Gao, L. Zhang, Y. Xie, C. Hu, Y. Zhang, L. Li, Y. Wang, C. Ma and P. Xu, *Bioresour. Technol.*, 2013, **137**, 111–115.

20 Y. He, F. Chen, M. Sun, H. Gao, Z. Guo, H. Lin, J. Chen, W. Jin, Y. Yang, L. Zhang and J. Yuan, *Molecules*, 2018, **23**, 619–634.

21 L. Li, Y. Wang, L. Zhang, C. Ma, A. Wang, F. Tao and P. Xu, *Bioresour. Technol.*, 2012, **115**, 111–116.

22 S. Ui, A. Mimura, M. Ohkuma and T. Kudo, *Lett. Appl. Microbiol.*, 1999, **28**, 457–460.

23 K. Goldberg, K. Schroer, S. Lütz and A. Liese, *Appl. Microbiol. Biotechnol.*, 2007, **76**, 249–255.

24 K. Liang and C. R. Shen, *Metab. Eng.*, 2017, **39**, 181–191.

25 Y. Wang, L. Li, C. Ma, C. Gao, F. Tao and P. Xu, *Sci. Rep.*, 2013, **3**, 2643.

26 J. Sambrook and D. W. Russell, *Molecular Cloning: A Laboratory Manual*, Clod Spring Harbor Laboratory, 3rd edn, 2001.

27 Y. J. Zhou, W. Yang, L. Wang, Z. Zhu, S. Zhang and Z. K. Zhao, *Microb. Cell Fact.*, 2013, **12**, 1–12.

28 S. J. Bae, S. Kim and J. S. Hahn, *Sci. Rep.*, 2016, **6**, 27667.

29 L. Zhang, Y. Y. Xu, J. Gao, H. Xu, C. Cao, F. Xue, G. Ding and Y. Y. Peng, *Bioresour. Technol.*, 2016, **201**, 319–328.

30 V. I. Tishkov and V. O. Popov, *Biomol. Eng.*, 2006, **23**, 89–110.

31 N. Samuel, T. Bao, X. Zhang, T. W. Yang, M. J. Xu, X. Li, I. Komera, T. Philibert and Z. M. Rao, *J. Chem. Technol. Biotechnol.*, 2017, **92**, 2477–2487.

32 R. Nina, N. Markus, L. Andreas, W. Roland, W. Andrea, E. Thorsten and H. Werner, *Biotechnol. Bioeng.*, 2010, **106**, 541–552.

33 A. E. Serov, A. S. Popova, V. V. Fedorchuk and V. I. Tishkov, *Biochem. J.*, 2002, **367**, 841–847.

34 J. Z. Lian, R. Chao and H. M. Zhao, *Metab. Eng.*, 2014, **23**, 92–99.

35 L. Zhang, Y. Zhang, Q. Liu, L. Meng, M. Hu, M. Lv, K. Li, C. Gao, P. Xu and C. Ma, *Sci. Rep.*, 2015, **5**, 9033.

36 K. Mädje, K. Schmölzer, B. Nidetzky and R. Kratzer, *Microb. Cell Fact.*, 2012, **11**, 1–8.

37 N. Z. Xie, H. Liang, R. B. Huang and P. Xu, *Biotechnol. Adv.*, 2014, **32**, 615–622.

38 Z. Liu, J. Qin, C. Gao, D. Hua, C. Ma, L. Li, Y. Wang and P. Xu, *Bioresour. Technol.*, 2011, **102**, 10741–10744.

39 M. Takeda, S. Anamizu, S. Motomatsu, X. Chen and C. R. Thapa, *Biosci. Biotechnol. Biochem.*, 2014, **78**, 1879–1886.